Jyväskylän yliopiston julkaisuarkisto
Jyväskylä University Digital Archive

UNIVERSITY OF JYVÄSKYLÄ

This is an electronic reprint of the original article.
This reprint *may differ* from the original in pagination and typographic detail.

Author(s): Liu, Jian; Jian, Nan; Ornelas, Isabel; Pattison, Alexander J.; Lahtinen, Tanja; Salorinne, Kirsi; Häkkinen, Hannu; Palmer, Richard E.

Title: Exploring the Atomic Structure of 1.8 nm Monolayer-Protected Gold Clusters with Aberration-Corrected STEM

Year: 2017

Version:

Please cite the original version:

Liu, J., Jian, N., Ornelas, I., Pattison, A. J., Lahtinen, T., Salorinne, K., Häkkinen, H., & Palmer, R. E. (2017). Exploring the Atomic Structure of 1.8 nm Monolayer-Protected Gold Clusters with Aberration-Corrected STEM. Ultramicroscopy, 176, 146-150. https://doi.org/10.1016/j.ultramic.2016.11.021

All material supplied via JYX is protected by copyright and other intellectual property rights, and duplication or sale of all or part of any of the repository collections is not permitted, except that material may be duplicated by you for your research use or educational purposes in electronic or print form. You must obtain permission for any other use. Electronic or print copies may not be offered, whether for sale or otherwise to anyone who is not an authorised user.

Author's Accepted Manuscript

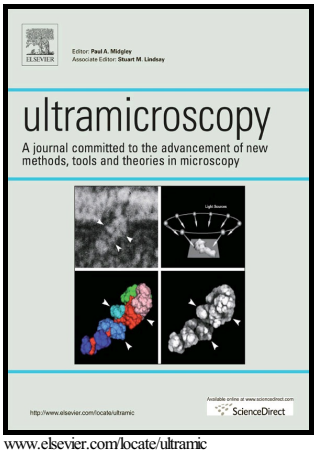

www.elsevier.com/locate/ultramic

Exploring the Atomic Structure of 1.8 nm Monolayer-Protected Gold Clusters with Aberration-Corrected STEM

Jian Liu, Nan Jian, Isabel Ornelas, Alexander J. Pattison, Tanja Lahtinen, Kirsi Salorinne, Hannu Häkkinen, Richard E. Palmer

PII: S0304-3991(16)30333-3
DOI: http://dx.doi.org/10.1016/j.ultramic.2016.11.021
Reference: ULTRAM12251

To appear in: *Ultramicroscopy*

Cite this article as: Jian Liu, Nan Jian, Isabel Ornelas, Alexander J. Pattison Tanja Lahtinen, Kirsi Salorinne, Hannu Häkkinen and Richard E. Palmer Exploring the Atomic Structure of 1.8 nm Monolayer-Protected Gold Cluster with Aberration-Corrected STEM, *Ultramicroscopy* http://dx.doi.org/10.1016/j.ultramic.2016.11.021

This is a PDF file of an unedited manuscript that has been accepted fo publication. As a service to our customers we are providing this early version o the manuscript. The manuscript will undergo copyediting, typesetting, an review of the resulting galley proof before it is published in its final citable form Please note that during the production process errors may be discovered whic could affect the content, and all legal disclaimers that apply to the journal pertain

ACCEPTED MANUSCRIPT

Exploring the Atomic Structure of 1.8 nm Monolayer-Protected Gold Clusters with Aberration-Corrected STEM

Jian Liu[a], Nan Jian[a], Isabel Ornelas[a], Alexander J. Pattison[a], Tanja Lahtinen[b], Kirsi Salorinne[b], Hannu Häkkinen[b,c], Richard E. Palmer[a]*

[a]Nanoscale Physics Research Laboratory, School of Physics and Astronomy, University of Birmingham, Birmingham, B15 2TT, UK.

[b]Department of Chemistry, [c] Department of Physics, Nanoscience Center, University of Jyväskylä, FI-40014 Jyväskylä, Finland

*R.E.Palmer@bham.ac.uk

Accepted manuscript

Abstract

Monolayer-protected (MP) Au clusters present attractive quantum systems with a range of potential applications e.g. in catalysis. Knowledge of the atomic structure is needed to obtain a full understanding of their intriguing physical and chemical properties. Here we employed aberration-corrected scanning transmission electron microscopy (ac-STEM), combined with multislice simulations, to make a round-robin investigation of the atomic structure of chemically synthesized clusters with nominal composition $Au_{144}(SCH_2CH_2Ph)_{60}$ provided by two different research groups. The MP Au clusters were "weighed" by the atom counting method, based on their integrated intensities in the high angle annular dark field (HAADF) regime and calibrated exponent of the Z dependence. For atomic structure analysis, we compared experimental images of hundreds of clusters, with atomic resolution, against a variety of structural models. Across the size range 123 to 151 atoms, only 3 percent of clusters matched the theoretically predicted

ACCEPTED MANUSCRIPT

$Au_{144}(SR)_{60}$ structure, while a large proportion of the clusters were amorphous (i.e. did not match any model structure). However, a distinct ring-dot feature, characteristic of local icosahedral symmetry, was observed in about 20% of the clusters.

1. Introduction

Monolayer-protected noble metal clusters are attracting considerable interest because of the appearance of magic numbers, which account for the stability of certain sizes, and their potential applications in bio-imaging, catalysis, sensors and so on [1-4]. Full atomic structure determination of these MP clusters is a key factor in understanding their physical and chemical properties in depth. For certain thiolated clusters, single crystal X-ray crystallography has provided reliable details of both the inner gold-core structures and the Au-S ligand units. To date the MP clusters identified by this method are $Au_{25}(SR)_{18}$ [5-7], $Au_{28}(SR)_{20}$ [8], $Au_{36}(SR)_{24}$ [9], $Au_{38}(SR)_{24}$ [10], $Au_{102}(SR)_{44}$ [11], $Au_{130}(SR)_{50}$ [12], and $Au_{133}(SR)_{52}$ [13, 14]. In the case of clusters of nominal composition $Au_{144}(SR)_{60}$, the determination of an ordered atomic structure with single crystal X-ray diffraction has so far proved unsuccessful, even though several research groups have obtained crystals [15-17]. This might be because the core and/or ligand layers of the clusters are amorphous [17], and/or because the crystals contain clusters of different sizes, for there are reports of many species of closely related composition, such as $Au_{144}(SR)_{59}$ [18], $Au_{146}(SR)_{59}$ [19], $Au_{137}(SR)_{56}$ [20, 21] etc. Recently, nominally $Au_{144}(SR)_{60}$ clusters doped with other metals (Ag [22-26], Pd [27], and Cu [28, 29]) have attracted attention due to their electronic and optical properties. Understanding of the $Au_{144}(SR)_{60}$ cluster is naturally of importance for further studies of these bimetallic clusters.

A theoretical structure for $Au_{144}(SR)_{60}$ was predicted by Lopez-Acevedo et al. [30] in 2009, and was composed of a chiral icosahedral Au_{114} core and 30 linear $Au(SR)_2$ units. Experimental studies by large angle X-ray diffraction (LA-XRD) [31, 32] extended X-ray absorption fine structure (EXAFS) [33] and ^1H NMR [34] techniques showed indirect evidence of agreement with

Accepted manuscript

ACCEPTED MANUSCRIPT

the proposed model. Nevertheless, the failure of single crystal X-ray experiments means that the precise structure of $Au_{144}(SR)_{60}$ remains unresolved.

Structure determination of MP Au clusters by electron microscopy is valuable, since it does not require the growth of high quality single crystals needed for single crystal X-ray crystallography. Nanobeam electron diffraction combined with HAADF-STEM imaging was employed to determine the structure of nominally $Au_{144}(SR)_{60}$ [35] and $Au_{130}(SR)_{50}$ [36] clusters by the Yacaman and Whetten groups. The experimental diffraction patterns and HAADF images show agreement with the predicted models [30, 37] in the case of specific individual clusters, but some other information, such as the cluster size distribution, percentage of clusters that fit the predicted model, and proportion of unidentified structures, is not given. Bruma et al [38] proposed a method of using scanning nanobeam diffraction to determine the structure of MP Au clusters ($Au_{102}(SR)_{44}$). They also reported the effect of electron beam damage of the clusters and found that the structure of thiolated clusters could be modified after a few seconds. Azubel et al [39] determined the structure of a MP Au_{68} cluster at atomic resolution by using low electron dose (~800 $e^-/Å^2$) TEM together with three-dimensional reconstruction of hundreds of TEM images. The advantage of this method, adapted from biological studies, is that the atomic structure of a MP Au cluster can in principle be revealed without any prior knowledge or fitting to model structures. However, this requires that the MP Au clusters should be homogenous both in structure and size. Statistical investigations of both cluster size and structure by HAADF-STEM have been reported by the Birmingham group, in the case of the MP Au_{38}, MP Au_{40} and MP Au_{55} clusters [40-43]. These experiments yielded the cluster nuclearity, aspect ratio, fluxionality and, in the case of MP Au_{55} [43], evidence that the atomic structure matches the theoretical prediction for one isolated size fraction.

Here we report a statistical round-robin investigation of nominally $Au_{144}(SR)_{60}$ clusters, synthesized independently by two different groups. The atom counting technique is conducted to determine the range of cluster sizes in the specimen, and the atomic structures are explored by

Accepted manuscript

ACCEPTED MANUSCRIPT

comparison with multislice simulations of different model structures. We find a very small fraction of clusters (~3%) match the theoretically predicted $Au_{144}(SR)_{60}$ structure [30], while a large proportion of the clusters are amorphous or unidentified. However, 20% of these clusters are found to exhibit ring-dot features in the atomic images, which is an indication of local icosahedral symmetry.

2. Experiments

MP Au clusters with (SCH_2CH_2Ph) ligands were synthesised at the University of Jyväskylä. The standard "MP Au_{144}" synthesis and corresponding ESI-MS analysis are reported in ref. [20], which showed the as-prepared sample to contain $Au_{144}(SR)_{60}$, but also $Au_{137}(SR)_{56}$ clusters. The clusters were sent to Birmingham in crystal form (shown in Figure 1a), and were then dissolved in toluene and drop cast onto a TEM grid covered with an amorphous carbon film. Single gold atoms were utilised as a mass balance to "weigh" the MP clusters via their integrated HAADF intensities, i.e., by the atom counting method [44-46]. HAADF-STEM atomic imaging was performed in a 200 kV JEM2100F STEM (JEOL) with spherical aberration probe corrector (CEOS). HAADF images were acquired with inner and outer detector angles of 62 and 164 mrad (camera length 10 cm), and probe convergence angle of 19 mrad. The scanning time for each frame was ~2.6 seconds and the electron dose was 7.9×10^4 $e^-/Å^2$/frame. The QSTEM software package [47] was utilised to simulate the HAADF images of candidate structures for comparison, an approach successfully applied to a range of size-selected Au clusters [48-50].

Accepted manuscript

3. Results and discussions

3.1 Size distribution and multislice simulations

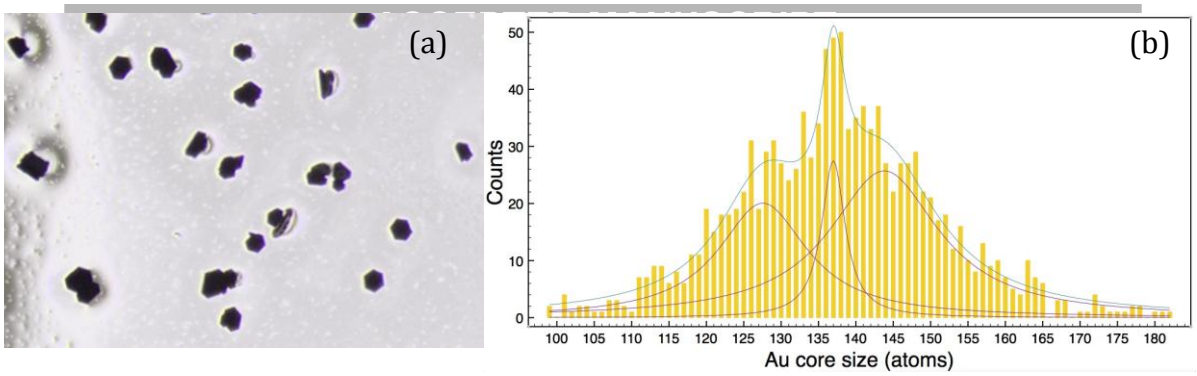

Fig 1 (a) Light microscopy image of crystals of MP Au clusters. Average size of the crystals was approximately 0.05 – 0.10 mm in diameter. (b) Au nuclearity for the MP Au clusters calibrated with HAADF intensity of single atoms by assuming each cluster has sixty (SCH_2CH_2Ph) ligands. A multiple Gaussian fit was applied.

In HAADF-STEM, the intensity of an atom is proportional to the atomic number to the power n (Z^n), where n= 1.46 ± 0.18 according to our previous calibration for the camera angle employed [51]. The HAADF intensity contributed by the nominal sixty (SCH_2CH_2Ph) ligands is then found equivalent to 17.9 ± 7.6 Au atoms. The Au core size (i.e. the total number of Au atoms including any in the $Au(SR)_2$ units) is then derived on the assumption (for convenience) that every MP cluster has sixty ligands. Single Au atoms are ejected by purposely scanning of a cluster for an extended time; an example of a HAADF-STEM image containing these reference single atoms is shown in Figure S1a. The integrated HAADF intensities of Au single atoms and undamaged MP clusters are shown in Figures S1b and S1c. Figure 1b shows the resulting histogram of Au atom numbers in the MP Au clusters obtained from this atom counting approach. The corresponding diameter distribution of the MP Au clusters is shown in Figure S1d; the average diameter of the clusters is 1.8 ± 0.1 nm. The average size of the MP clusters is 137 ± 11 Au atoms, rather than 144. The size distribution is broad and for the purpose of illustration (only), we also show in Figure 1b a multiple Gaussian fit with three peaks at 128 ± 7, 137 ± 2 and 144 ± 9. The fit is chosen because it is compatible with the electrospray ionization (ESI) mass spectrum in ref. [20], in which both $Au_{144}(SR)_{60}$ and $Au_{137}(SR)_{56}$ peaks are identified. The existence of clusters at the peak of 128, may

Accepted manuscript

ACCEPTED MANUSCRIPT

be because of losing a number of $Au_4(SR)_4$ fragments, which was observed in the MALDI mass spectrum[52]. The size distribution of Figure 1b indicates that the sample synthesised contains different size clusters, although it can still form crystals. This may well explain why well-defined single crystal X-ray diffraction patterns have not been obtained for nominal $Au_{144}(SR)_{60}$ single crystals.

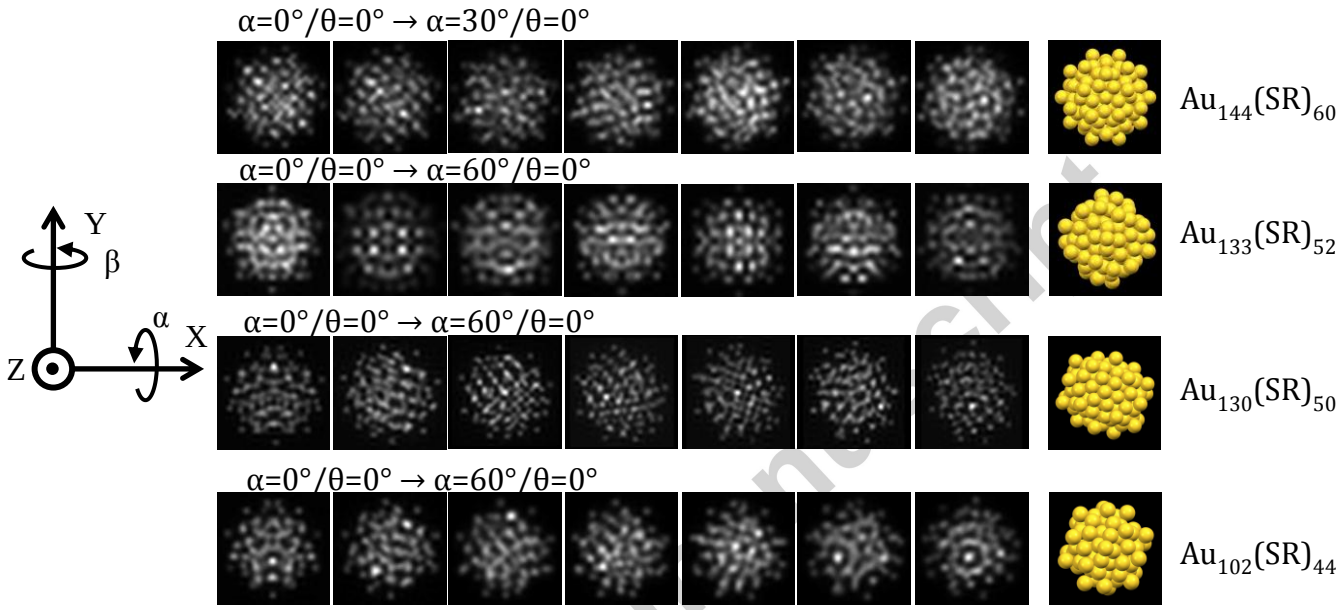

Fig 2 Atomic models and multislice simulations examples of $Au_{144}(SR)_{60}$, $Au_{133}(SR)_{52}$, $Au_{130}(SR)_{50}$ and $Au_{102}(SR)_{44}$. The ligands are not shown. Z-axis is parallel to the view direction.

The structural identification of the MP Au clusters was performed by comparing the experimental images with multislice simulations. Even clusters of a single isomer deposited on the carbon film of a TEM grid would have random orientations and thus present a variety of projection patterns in HAADF-STEM images. Therefore, a "simulation atlas" which covers the full range of orientations was calculated for each candidate cluster structure investigated. Considering the experimental size range of the clusters in Figure 1b, models of $Au_{102}(SR)_{44}$ [11], $Au_{130}(SR)_{50}$ [37], $Au_{133}(SR)_{52}$ [14], and $Au_{144}(SR)_{60}$ [30] were chosen for comparison with the experimental images. These cluster models have either been theoretically proposed [37, 30] or experimentally

ACCEPTED MANUSCRIPT

measured [11, 14]. Figure 2 shows some examples of simulations based on the models. The simulation atlases are presented in detail in Figures S6-S11.

3.2 Atomic structure investigation

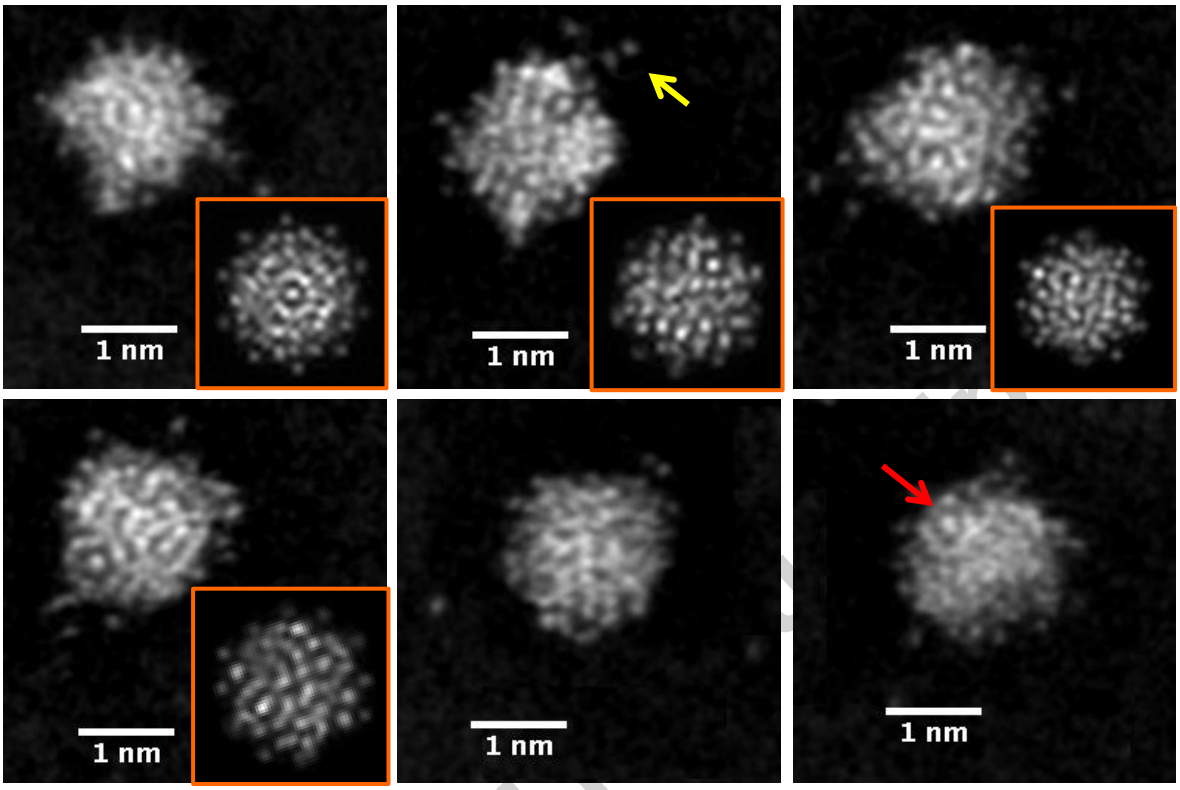

Fig 3 (a-f) are HAADF-STEM images of MP Au clusters. (a-d) are MP Au clusters found to be similar to the $Au_{144}(SR)_{60}$ model. Examples of ejected atoms are indicated with a yellow arrow. The insets are the corresponding simulations along the orientations of (a) α=40°, β=70°; (b) α=20°, β=50°; (c) α=15°, β=20°; (d) α=10°, β=30°. (e) An example of unidentified cluster and (f) a cluster with a ring-dot feature (as indicated by the red arrow).

The comparison with the simulations was carried out for 849 experimental cluster images. This systematic investigation demonstrates that only about 3% of the clusters match the predicted $Au_{144}(SR)_{60}$ structure [30]. (Even if we restrict analysis to clusters in the size fraction 139 to 149 Au atoms, only 4% of the experimental images match the theoretical structure.) The fraction of images, which matches the other models, is even lower. Idealised bare Au_{147} (no ligands) clusters

ACCEPTED MANUSCRIPT

with icosahedral, decahedral and face-centred cubic structures were also used for comparison. They are not explicit in the paper because of the low match to the simulations and the fact that they were not ligand-protected. Figures 3(a-d) show some examples of HAADF-STEM images of the MP Au clusters that are found to fit the $Au_{144}(SR)_{60}$ simulations. As we can see that the main motif in these clusters (ring-dot or straight line features) is in line with the simulations (including the location of the motif). However, the matches between experiment and simulation are not perfect at the detailed level. This deviation may arise because of instability of the clusters, at the atomic level, under the electron beam irradiation. Firstly, radiation-induced atom diffusion [53] may cause atom smearing during image acquisition. Secondly, the surface structure of thiolated clusters is expected to be sensitive to the state of the ligands [54, 55], so any radiation damage to the ligands may induce cluster structure modification. Thirdly, less strongly bound Au atoms can be ejected during a normal imaging scan, as we observe individual atoms a few angstroms away from the cluster (indicated with the yellow arrow in Figure 3b). However, our previous study on MP Au_{55} [43] clusters found that over 40% of the cluster images matched the simulations. Thus we think that the electron beam has a limited effect on the core structure of the clusters. Additionally, the $Au_{144}(SR)_{60}$ cluster may have several possible isomeric structures of similar energy. Tian et al [56] showed two isomers of $Au_{38}(SR)_{24}$ and the less stable isomer transformed irreversibly to the more stable isomer when heated to 50 °C. These four reasons may explain the imperfect detailed match between experimental and simulated cluster structure, even in generally well-matched cases.

Most of the cluster images were found to be amorphous (Figure 3e). However, amongst these clusters, we found that a good proportion (~20%) of clusters presented ring-dot features, as highlighted in Figure 3f. To check the generality of our result, in addition to the MP Au cluster crystals from Jyväskylä, we also explored a batch of nominally $Au_{144}(SR)_{60}$ clusters (with ligands of SCH_2CH_2Ph) synthesised by the group of Prof. A. Dass of the University of Mississippi. The standard "MP Au_{144}" synthesis and corresponding MALDI-MS analysis (Figure S2) are reproduced

Accepted manuscript

ACCEPTED MANUSCRIPT

in the electronic supplementary information. The HAADF-STEM imaging conditions employed for these powder samples were the same as the sample described above. The size distribution (Figure S3, 4) and structure comparison (Figure S5) are shown in the Supporting Information. We found that about 7% of the cluster images were similar to the predicted $Au_{144}(SR)_{60}$ model and that an additional ~30% cluster images presented ring-dot features. These results are similar to those for the Jyväskylä sample. The appearance of this feature is consistent with the existence of local icosahedral symmetry in the clusters. A simulation atlas of an icosahedral bare Au_{147} is presented in Figure S12. The ring-dot feature can be seen in the simulations of $Au_{144}(SR)_{60}$ (Figure S6-7), and $Au_{133}(SR)_{52}$ (Figure S11) as well as $Au_{102}(SR)_{44}$ (Figure S8) and $Au_{130}(SR)_{50}$ (Figure S9-10). Both $Au_{102}(SR)_{44}$ and $Au_{130}(SR)_{50}$ have decahedral cores, but those are encapsulated by two five-fold symmetry caps [11,37] and a ring-dot feature occurs at certain orientations in the simulations. Thus the observed ring-dot motifs may be traceable either to an icosahedral core or, in a few cases, to a five-fold cap. Worth noting is that not all of the orientations show a ring-dot feature, so a higher percentage of clusters may contain similar structural elements. For example, in the case of $Au_{144}(SR)_{60}$and $Au_{133}(SR)_{52}$, if 20% of the images present a ring-dot feature, and assume the clusters are randomly orientated, then 40% of the clusters may contain an icosahedral core (around 50% of atlas simulations present the ring-dot feature).

Accepted manuscript

4. Conclusion

In summary, we have employed aberration-corrected STEM to characterise the size and provide insights into the structure of nominally $Au_{144}(SR)_{60}$ clusters. We find the samples synthesised contain a range of cluster sizes, which is also indicated in the mass spectra. Image comparison with multislice simulations of model structures of all orientations shows that only about 3% of clusters fit the predicted $Au_{144}(SR)_{60}$ structure. Nevertheless, the experimental images exhibited a ring-dot feature, characteristic of local icosahedral order, in a further 20 to 30% of clusters. Based

ACCEPTED MANUSCRIPT

on the simulation atlases, it may be that an even higher proportion of clusters, perhaps 40%, contain icosahedral elements. Electron beam damage at the atomic scale may account for the imperfect matches between simulations and experiments, and no doubt both low doses and low beam energy would be desirable for minimising the electron beam effect on the thiolated clusters, but there is no doubt that the ability of HAADF-STEM both to size and to analyse individual clusters is a powerful tool in the structure resolution problem. In the present case, the rather broad size distribution obtained from the atom counting is consistent with the absence of well-ordered X-ray diffraction patterns from the cluster crystals.

Acknowledgements

We are grateful to Dr. Simon Plant for deposition of the $Au_{923\pm23}$ clusters and to Prof. Amala Dass for providing the monolayer-protected gold clusters. We thank the EPSRC for financial support. The STEM instrument employed in this research was obtained through the Birmingham Science City project "Creating and Characterising Next Generation Advanced Materials," supported by Advantage West Midlands (AWM) and funded in part by the European Regional Development Fund (ERDF).

Accepted manuscript

References

[1] T. Tsukuda, H. Häkkinen, Protected Metal Clusters: From Fundamentals to Applications, Elsevier, Amsterdam, 2015.

[2] L. Polavarapu, M. Manna, Q. Xu, Biocompatible Glutathione Capped Gold Clusters as One- and Two-Photon Excitation Fluorescence Contrast Agents for Live Cells Imaging, Nanoscale 3 (2011) 429-434.

ACCEPTED MANUSCRIPT

[3] G. Ma, A. Binder, M. Chi, C. Liu, R. Jin, D. Jiang, J. Fan, S. Dai, Stabilizing Gold Clusters by Heterostructured Transition-Metal Oxide-Mesoporous Silica Supports for Enhanced Catalytic Activities for CO Oxidation, Chem. Commun. 48 (2012) 11413–11415.

[4] A. Shivhare, S. J. Ambrose, H. Zhang, R.W. Purves, R.W.J. Scott, Stable and Recyclable Au_{25} Clusters for the Reduction of 4-Nitrophenol, Chem. Commun. 49 (2013) 276–278.

[5] M.W. Heaven, A. Dass, P.S. White, K.M. Holt, R.W. Murray, Crystal Structure of the Gold Nanoparticle $[N(C_8H_{17})_4][Au_{25}(SCH_2CH_2Ph)_{18}]$, J. Am. Chem. Soc. 130 (2008) 3754–3755.

[6] M. Zhu, C.M. Aikens, F.J. Hollander, G.C. Schatz, R. Jin, Correlating the Crystal Structure of a Thiol-Protected Au_{25} Cluster and Optical Properties, J. Am. Chem. Soc. 130 (2008) 5883–5885.

[7] M. Zhu, W.T. Eckenhoff, T. Pintauer, R. Jin, Conversion of Anionic $[Au_{25}(SCH_2CH_2Ph)_{18}]^-$ Cluster to Charge Neutral Cluster via Air Oxidation, J. Phys. Chem. C 112 (2008) 14221–14224.

[8] C. Zeng, T, Li, A. Das, N.L. Rosi, R. Jin, Chiral Structure of Thiolate-Protected 28-Gold-Atom Nanocluster Determined by X-ray Crystallography, J. Am. Chem. Soc. 135 (2013) 10011–10013.

[9] C. Zeng, H. Qian, T. Li, G. Li, N.L. Rosi, B. Yoon, R.N. Barnett, R.L. Whetten, U. Landman, R. Jin, Total Structure and Electronic Properties of the Gold Nanocrystal $Au_{36}(SR)_{24}$, Angew. Chem. Int. Ed. 51 (2012) 13114–13118.

[10] H. Qian, W.T. Eckenhoff, Y. Zhu, T. Pintauer, R. Jin, Total Structure Determination of Thiolate-Protected Au_{38} Nanoparticles, J. Am. Chem. Soc. 132 (2010) 8280–8281.

[11] P.D. Jadzinsky, G. Calero, C.J. Ackerson, D.A. Bushnell, R.D. Kornberg, Structure of a Thiol Monolayer-Protected Gold Nanoparticle at 1.1 Å Resolution, Science 318 (2007) 430–433.

[12] Y. Chen, C. Zeng, C. Liu, K. Kirschbaum, C. Gayathri, R.R. Gil, N.L. Rosi, R. Jin, Crystal Structure of Barrel-Shaped Chiral $Au_{130}(P\text{-}MBT)_{50}$ Nanocluster, J. Am. Chem. Soc. 137 (2015) 10076–10079.

[13] C. Zeng, Y. Chen, K. Kirschbaum, K. Appavoo, M.Y. Sfeir, R. Jin, Structural Patterns at All Scales in a Nonmetallic Chiral $Au_{133}(SR)_{52}$ Nanoparticle, Sci. Adv. 1 (2015) e1500045.

Accepted manuscript

ACCEPTED MANUSCRIPT

[14] A. Dass, S. Theivendran, P.R. Nimmala, C. Kumara, V.R. Jupally, A. Fortunelli, L. Sementa, G. Barcaro, X. Zuo, B.C. Noll, $Au_{133}(SPh\text{-}tBu)_{52}$ Nanomolecules: X-Ray Crystallography, Optical, Electrochemical, and Theoretical Analysis, J. Am. Chem. Soc. 137 (2015) 4610–4613.

[15] T.G. Schaaff, M.N. Shafigullin, J.T. Khoury, I. Vezmar, R.L. Whetten, Properties of a Ubiquitous 29 kDa Au:SR Cluster Compound, J. Phys. Chem. B 105 (2001) 8785–8796.

[16] C.J. Ackerson, P.D. Jadzinsky, J.Z. Sexton, D.A. Bushnell, R.D. Kornberg, Synthesis and Bioconjugation of 2 and 3 nm-Diameter Gold Nanoparticles, Bioconjugate Chem. 21 (2010) 214–218.

[17] J. Koivisto, K. Salorinne, S. Mustalahti, T. Lahtinen, S. Malola, M. Pettersson, Vibrational Perturbations and Ligand–Layer Coupling in a Single Crystal of $Au_{144}(SC_2H_4Ph)_{60}$ Nanocluster, J. Phys. Chem. Lett. 144 (2014) 1–6.

[18] N.K. Chaki, Y. Negishi, H. Tsunoyama, Y. Shichibu, T. Tsukuda, Ubiquitous 8 and 29 kDa Gold: alkanethiolate Cluster Compounds: Mass-Spectrometric Determination of Molecular Formulas and Structural Implications, J. Am. Chem. Soc. 130 (2008) 8608–8610.

[19] C.A. Fields-zinna, R. Sardar, C.A. Beasley, R.W. Murray, N. Carolina, Electrospray Ionization Mass Spectrometry of Intrinsically Cationized Nanoparticles, $[Au_{144/146}(SC_{11}H_{22}N(CH_2CH_3)_3{}^+)_x(S(CH_2)_5CH_3)_y]^{x+}$, J. AM. Chem. Soc. 146 (2009) 16266–16271.

[20] K. Salorinne, T. Lahtinen, J. Koivisto, E. Kalenius, M. Nissinen, M. Pettersson, H. Häkkinen, Non-destructive Size Determination of Thiol-Stabilized Gold Nanoclusters in Solution by Diffusion Ordered NMR Spectroscopy, Anal. Chem. 85 (2013) 3489–3492.

[21] V.R. Jupally, A.C. Dharmaratne, D. Crasto, A.J. Huckaba, C. Kumara, P.R. Nimmala, N. Kothalawala, J.H. Delcamp, A. Dass, $Au_{137}(SR)_{56}$ Nanomolecules: Composition, Optical Spectroscopy, Electrochemistry and Electrocatalytic Reduction of CO_2, Chem. Commun. 50 (2014) 9895–9898.

[22] C. Kumara, A. Dass, $(AuAg)_{144}(SR)_{60}$ Alloy Nanomolecules, Nanoscale 3 (2011) 3064–3067.

Accepted manuscript

ACCEPTED MANUSCRIPT

[23] S. Malola, H. Häkkinen, Electronic Structure and Bonding of Icosahedral Core Shell Gold-Silver Nanoalloy Clusters $Au_{144-x}Ag_x(SR)_{60}$, J. Phys. Chem. Lett. 2 (2011) 2316–2321.

[24] J. Koivisto, S. Malola, C. Kumara, A. Dass, M. Pettersson, Experimental and Theoretical Determination of the Optical Gap of the $Au_{144}(SC_2H_4Ph)_{60}$ Cluster and the $(Au/Ag)_{144}(SC_2H_4Ph)_{60}$ Nanoalloys, J. Phys. Chem. Lett. 3 (2012) 3076-3080.

[25] S. Malola, L. Lehtovaara, H. Häkkinen, TDDFT Analysis of Optical Properties of Thiol Monolayer-Protected Gold and Intermetallic Silver–Gold $Au_{144}(SR)_{60}$ and $Au_{84}Ag_{60}(SR)_{60}$ Clusters, J. Phys. Chem. C 118 (2014) 20002–20008.

[26] G. Barcaro, L. Sementa, A. Fortunelli, M. Stener, Comment on "$(Au–Ag)_{144}(SR)_{60}$ Alloy Nanomolecules" by C. Kumara and A. Dass, Nanoscale, 2011, 3 , 3064, Nanoscale 7 (2015) 8166–8167.

[27] N. Kothalawala, C. Kumara, R. Ferrando, A. Dass, $Au_{144-x}Pd_x(SR)_{60}$ Nanomolecules, Chem. Commun. 49 (2013) 10850-10852.

[28] A.C. Dharmaratne, A. Dass, $Au_{144-x}Cu_x(SC_6H_{13})_{60}$ Nanomolecules: Effect of Cu Incorporation on Composition and Plasmon-like Peak Emergence in Optical Spectra, Chem. Commun. 50 (2014) 1722–1724.

[29] S. Malola, M.J. Hartmann, H. Häkkinen, Copper Induces a Core Plasmon in Intermetallic $Au_{(144,145)-X}Cu_X(SR)_{60}$ Nanoclusters, J. Phys. Chem. Lett. 6 (2015) 515–520.

[30] O. Lopez-acevedo, J. Akola, R.L. Whetten, H. Grönbeck, H. Häkkinen, Structure and Bonding in the Ubiquitous Icosahedral Metallic Gold Cluster $Au_{144}(SR)_{60}$, J. Phys. Chem. C 144 (2009) 5035–5038.

[31] C.L. Cleveland, U. Landman, T.G. Schaaff, M.N. Shafigullin, P.W. Stephens, R.L. Whetten, Structural Evolution of Smaller Gold Nanocrystals: The Truncated Decahedral Motif, Phys. Rev. Lett. 79 (1997) 1873–1876.

Accepted manuscript

ACCEPTED MANUSCRIPT

[32] T.G. Schaaff, M.N. Shafigullin, J.T. Khoury, I. Vezmar, R.L. Whetten, W.G. Cullen, P.N. First, C. Gutiérrez-Wing, J. Ascensio, M. Jose-Yacamán, Isolation of Smaller Nanocrystal Au Molecules: Robust Quantum Effects in Optical Spectra, J. Phys. Chem. B 101 (1997) 7885–7891.

[33] M.A. MacDonald, P. Zhang, H. Qian, R. Jin, Site-Specific and Size-Dependent Bonding of Compositionally Precise Gold–Thiolate Nanoparticles from X-Ray Spectroscopy, J. Phys. Chem. Lett. 1 (2010) 1821–1825.

[34] O.A. Wong, C.L. Heinecke, A.R. Simone, R.L. Whetten, C.J. Ackerson, Ligand Symmetry-Equivalence on Thiolate Protected Gold Nanoclusters Determined by NMR Spectroscopy, Nanoscale 4 (2012) 4099–4102.

[35] D. Bahena, N. Bhattarai, U. Santiago, A. Tlahuice, A. Ponce, S.B.H. Bach, B. Yoon, R.L. Whetten, U. Landman, M. Jose-Yacamán, STEM Electron Diffraction and High-Resolution Images Used in the Determination of the Crystal Structure of the $Au_{144}(SR)_{60}$ Cluster, J. Phys. Chem. Lett. 4 (2013) 975–981.

[36] A. Tlahuice-flores, U. Santiago, D. Bahena, E. Vinogradova, C.V. Conroy, T. Ahuja, S.B.H. Bach, A. Ponce, G. Wang, M. Jose-Yacamán, R.L. Whetten, Structure of the Thiolated Au_{130} Cluster, J. Phys. Chem. A 117 (2013) 10470–10476.

[37] Y. Negishi, C. Sakamoto, O. Tatsuya, T. Tsukuda, Synthesis and the Origin of the Stability of Thiolate-Protected Au_{130} and Au_{187} Clusters, J. Phys. Chem. Lett. 3 (2012) 1624–1628.

[38] A. Bruma, U. Santiago, D. Alducin, G.P. Villa, R.L. Whetten, A. Ponce, M. Mariscal, M. José-Yacamán, Structure Determination of Superatom Metallic Clusters Using Rapid Scanning Electron Diffraction, J. Phys. Chem. C 102 (2015) 1902–1908.

[39] M. Azubel, J. Koivisto, S. Malola, D. Bushnell, G.L. Hura, A.L. Koh, H. Tsunoyama, T. Tsukuda, M. Pettersson, H. Häkkinen, R.D. Kornberg, Electron Microscopy of Gold Nanoparticles at Atomic Resolution, Science 345 (2014) 909–912.

Accepted manuscript

ACCEPTED MANUSCRIPT

[40] Z.W. Wang, O. Toikkanen, B.M. Quinn, R.E. Palmer, Real-Space Observation of Prolate Monolayer-Protected Au_{38} Clusters Using Aberration-Corrected Scanning Transmission Electron Microscopy, Small 7 (2011) 1542–1545.

[41] S. Malola, L. Lehtovaara, S. Knoppe, K.J. Hu, R.E. Palmer, T. Bürgi, H. Häkkinen, $Au_{40}(SR)_{24}$ Cluster as A Chiral Dimer of 8-Electron Superatoms: Structure and Optical Properties, J. Am. Chem. Soc. 134 (2012) 19560–19563.

[42] Z.W. Wang, O. Toikkanen, F. Yin, Z.Y. Li, B.M. Quinn, R.E. Palmer, Counting the Atoms in Supported, Monolayer-Protected Gold Clusters, J. Am. Chem. Soc. 132 (2010) 2854–2855.

[43] N. Jian, C. Stapelfeldt, K.J. Hu, M. Fröba, R.E. Palmer, Hybrid Atomic Structure of the Schmid Cluster $Au_{55}(PPh_3)_{12}Cl_6$ Resolved by Aberration-Corrected STEM, Nanoscale 7 (2015) 885–888.

[44] Z.W. Wang, Z.Y. Li, S.J. Park, A. Abdela, D. Tang, R.E. Palmer, Quantitative Z-Contrast Imaging in the Scanning Transmission Electron Microscope with Size-Selected Clusters, Phys. Rev. B 84 (2011) 073408.

[45] N. Young, Z.Y. Li, Y. Chen, S. Palomba, M. Di Vece, R.E. Palmer, Weighing Supported Nanoparticles: Size-Selected Clusters as Mass Standards in Nanometrology, Phys. Rev. Lett. 101 (2008) 246103.

[46] D. Pearmain, S.J. Park, Z.W. Wang, A. Abdela, R.E. Palmer, Z.Y. Li, Size and Shape of Industrial Pd Catalyst Particles Using Size-Selected Clusters as Mass Standards, Appl. Phys. Lett. 102 (2013) 163103.

[47] C. Koch, Determination of Core Structure Periodicity and Point Defect Density Along Dislocations, Ph.D. Thesis, Arizona State University, Arizona, 2002.

[48] D.M. Wells, G. Rossi, R. Ferrando, R.E. Palmer, Metastability of the Atomic Structures of Size-Selected Gold Nanoparticles, Nanoscale 7 (2015) 6498–6503.

[49] Z.W. Wang, R.E. Palmer, Direct Atomic Imaging and Dynamical Fluctuations of the Tetrahedral Au_{20} Cluster, Nanoscale 4 (2012) 4947–4949.

Accepted manuscript

ACCEPTED MANUSCRIPT

[50] Z.W. Wang, R.E. Palmer, Atomic-Scale Structure Analysis by Advanced Transmission Electron Microscopy, in: T. Tsukuda, H. Häkkinen (Eds), Protected Metal Clusters: From Fundamentals to Applications", Frontiers of Nanoscience, 2015, pp. 127–159.

[51] Z.W. Wang, R.E. Palmer, Intensity Calibration and Atomic Imaging of Size-Selected Au and Pd Clusters in Aberration-Corrected HAADF-STEM, J. Phys. Conf. Ser. 371 (2012) 012010.

[52] A. Dass, Nano-scaling law: geometric foundation of thiolated gold nanomolecules, Nanoscale, 4 (2012) 2260–2263.

[53] R.F. Egerton, R. McLeod, F. Wang, M. Malac, Basic Questions Related to Electron-Induced Sputtering in the TEM, Ultramicroscopy 110 (2010) 991–997.

[54] C. Zeng, Y. Chen, A. Das, R. Jin, Transformation Chemistry of Gold Nanoclusters: From One Stable Size to Another, J. Phys. Chem. Lett. 6 (2015) 2976–2986.

[55] Y. Chen, C. Zeng, D.R Kauffman, R. Jin, Tuning the Magic Size of Atomically Precise Gold Nanoclusters via Isomeric Methylbenzenethiols, Nano Lett. 15 (2015) 3603–3609.

[56] S. Tian, Y.Z. Li, M.B. Li, J. Yuan, J. Yang, Z. Wu, R. Jin, Structural Isomerism in Gold Nanoparticles Revealed by X-Ray Crystallography, Nat. Commun. 6 (2015) 8667.

Highlights

- The monolayer-protected gold clusters with nominal composition $Au_{144}(SCH_2CH_2Ph)_{60}$ synthesized by two different research groups were "weighed" by the atom counting method;
- Atomic structure comparison with multislice simulations of model structures of all orientations shows a few percentage of clusters fit the predicted $Au_{144}(SR)_{60}$ structure.
- A ring-dot feature, characteristic of local icosahedral order, was frequently observed in the experimental images.

Accepted manuscript